Hindawi
Complexity
Volume 2017, Article ID 7015243, 8 pages
https://doi.org/10.1155/2017/7015243

Research Article

Cascade-Driven Series with Narrower Multifractal Spectra Than Their Surrogates: Standard Deviation of Multipliers Changes Interactions across Scales

Jun Taek Lee and Damian G. Kelty-Stephen

Grinnell College, 1115 8th Ave., No. 3846, Grinnell, IA 50112, USA

Correspondence should be addressed to Jun Taek Lee; leejunta@grinnell.edu

Received 22 July 2016; Revised 10 December 2016; Accepted 18 December 2016; Published 15 January 2017

Academic Editor: Roberto Natella

Multifractal (or singularity) spectra widths w allow diagnosing cascade structure through comparing original series' widths w_{Orig} to surrogate series' widths w_{Surr}. However, interpretations of $0 < w_{\text{Orig}} < w_{\text{Surr}}$ have been ambiguous. Stochastic multipliers generate cascades with $0 < w_{\text{Orig}} < w_{\text{Surr}}$ by diversifying cross-scale interactions using white-noise multipliers. Multifractal detrended fluctuation analysis (MF-DFA) and Chhabra and Jensen's method provided two estimates of w_{Orig} for 200 simulated series at each value $0.1 \leq \sigma \leq 1.1$ incrementing by 0.05. Increasing σ draws w_{Orig} away from $w_{\text{Surr}} < w_{\text{Orig}}$ and towards $0 < w_{\text{Orig}} < w_{\text{Surr}}$ for both methods but more for MF-DFA. $0 < w_{\text{Orig}} < w_{\text{Surr}}$ indicates cascades with cross-scale interactions more diverse than in cascades with $w_{\text{Surr}} < w_{\text{Orig}}$.

1. Introduction

Multifractal analysis provides an elegant test for cascade structure in empirical series [1–3]. Cascades are nonlinear processes involving iterative branching, splitting, or aggregating structures across repeated generations [4–6]. Multifractal analysis computes a spectrum of singularity strengths governing power-law growth relative to measurement scale. Width of this multifractal (or singularity) spectrum w varies with the number of estimable power-law relationships. w depends on the strength of cascade-like interactions across scales [7].

1.1. Surrogate Comparison. w is, however, not a transparent window onto cascade-like interactivity across scales. Surrogate testing is as necessary for proper interpretation of w as for any nonlinear metric [8–11]. Linear features of a measurement series spuriously increase w. The sources of multifractality are first nonlinear correlations and second PDF and linear correlations [12, 13]. The former source indicates cascade-like origins, and the latter does not. Multifractal diagnosis of cascade structure requires comparison of original measurement series' multifractal-spectrum width w_{Orig} to w_{Surr}, the width for surrogates matching mean, variance, and autocorrelation function of the original series. The current preferred surrogate algorithm is the Iterative Amplitude Adjusted Fourier Transform (IAAFT) algorithm preserving linear properties while randomizing phase by shuffling the order of values in original series. Because skewed histograms alone can inflate w_{Orig} [14], IAAFT surrogates need not generate nonzero w_{Surr}. The present article addresses the issue of interpreting the result of $0 < w_{\text{Orig}} < w_{\text{Surr}}$.

1.2. The Problem. To our knowledge, diagnosing cascade-like interactions across scales using multifractal analysis is a simple dichotomy: evidence for cascades or not. The problem is that interpretations vary particularly for diagnosing those cases in which $0 < w_{\text{Orig}} < w_{\text{Surr}}$. According to some [15], $0 < w_{\text{Orig}} < w_{\text{Surr}}$ entails the notion that the original series is monofractal, and cascade structure gives rise only to $w_{\text{Surr}} < w_{\text{Orig}}$. Other interpretations have presumed that $0 \neq w_{\text{Orig}} \neq w_{\text{Surr}}$ indicates nonlinear temporal structure [1, 16–19].

We offer the present simulation work, first, to demonstrate that extremely simple cascades do generate $0 < w_{\text{Orig}} < w_{\text{Surr}}$ and, second, to present a manipulation of interactions

across time scales in these cascades warranting a more bidirectional, more continuous interpretation of the cascade structure when $0 \neq w_{\text{Orig}} \neq w_{\text{Surr}}$. The next section briefly reviews binomial cascades as well as our manipulation of multipliers in this two-daughter-cascade framework.

1.3. Cascades. Cascades are iterative manipulations of n_g cells over g generations that may redistribute the proportion $p_{i,j}$ contained in each ith parent cell in generation j (for $j < g, i < n_j$) across some number of daughter cells in generation $j+1$ each containing $p_{k,j+1}$, for $1 \leq k \leq n_{j+1}$. For instance, the standard binomial multiplicative cascade [20] begins with a single cell containing unit proportion $p_{1,1}$ and proceeds by fragmenting this unit proportion unevenly, such that the subsequent generation contains two daughter cells $p_{1,2}$ and $p_{2,2}$, such that $p_{1,2} \neq p_{2,2}$ and $p_{1,2}/p_{2,2} = c$, where c is a constant. This constant ratio c defines all parent-to-daughter cell relationships across all generations; that is, for any parent cell containing proportion $p_{i,j}$ in generation j of the binomial multiplicative cascade, the daughter cells appearing in the next generation $j+1$ will contain proportions $p_{2i-1,j+1} = c \times p_{i,j}/(c+1)$ and $p_{2i,j+1} = p_{i,j}/(c+1)$ in the same sequence across the entire generation. Hence, the binomial multiplicative cascade uses the deterministic multipliers $c/(c+1)$ and $1/(c+1)$.

Our simulations of cascade processes involve the same splitting of parent cells into two daughter cells. A key difference in our approach is the use of stochastic multipliers. Instead of using constant c to define unevenness of proportion p across daughter cells, we generated a new additive Gaussian white-noise x process to specify each new generation; that is, to redistribute proportions contained by n_j parent cells in generation j, we defined $x_{k,j+1}$ as a vector of length $2n_j = n_{j+1}$, where $1 \leq k \leq n_{j+1}$ are numbers randomly selected from a Gaussian distribution, and these random numbers served as multipliers to specify the proportion contained in each daughter cell. For parent cells containing proportion $p_{i,j}$, the two resulting daughter cells would contain proportion $p_{2i-1,j+1} = x_{2i-1,j+1} \times p_{i,j}$ and proportion $p_{2i,j+1} = x_{2i,j+1} \times p_{i,j}$. What we held constant across generations was the mean of 1 and standard deviation σ for all rows in x.

Our general hypothesis is that replacing the constant multipliers defined by the constant ratio c with stochastic multipliers x in a similar two-daughter framework might provide one way to reduce w_{Orig} into the range $0 < w_{\text{Orig}} < w_{\text{Surr}}$. Completely even splitting of proportion from parent to daughter cells would produce a cascade of ideally monofractal structure (i.e., the Cantor set), $w_{\text{Orig}} = 0$. It is the deterministic, repeating pattern of unevenness of the constant multipliers across daughter cells that makes the monofractal cascade multifractal with $0 < w_{\text{Orig}}$. So, we suspect that stochastic multipliers might at once provide the heterogeneity to produce a multifractal cascade but also randomize the heterogeneity to deterministically favor neither the first nor the second daughter of each parent cell with greater proportion. Whereas the binomial multiplicative cascade enforces the same pattern through all interactions across all scales, stochastic multipliers might make interactions across the scales of resulting cascades more divergent.

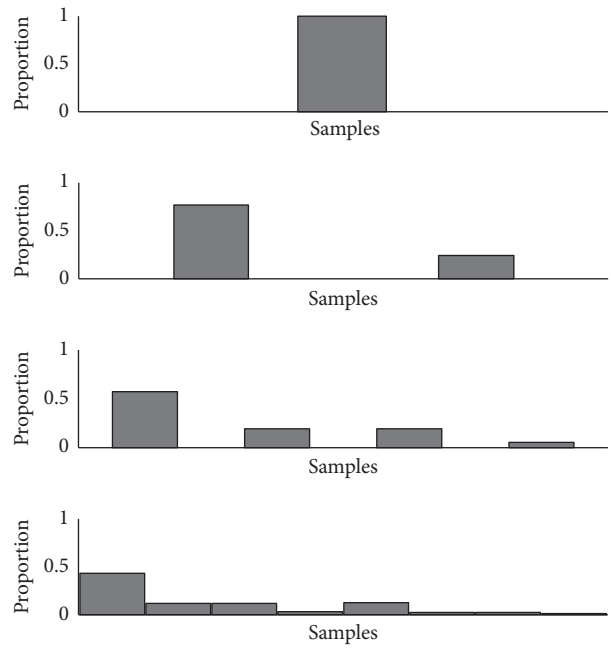

Figure 1: Schematic of binomial multiplicative cascade with four generations.

The sense in which we envision this divergence has to do with our hope that the promise of "interactions across scales" in cascade-generated series should maintain all the same promise of earlier claims regarding nonlinearity. Because linearity entails an expectation of symmetry across time, nonlinearity opens the door to asymmetries which might unfold across any of many directions across time. This issue motivates the two-sided comparison, that is, $0 \neq w_{\text{Orig}} \neq w_{\text{Surr}}$, of series against linear surrogates: we should not merely test whether metrics from "nonlinear" analyses (e.g., w) exceed values computed for linear surrogates. From the baseline nonzero multifractal-spectrum width due to histogram skew, nonlinear interactions across time might be just as likely to narrow the spectrum width towards $0 < w_{\text{Orig}} < w_{\text{Surr}}$ as to widen it towards $w_{\text{Surr}} < w_{\text{Orig}}$. Nonlinearity might violate time symmetry through constricting or amplifying complexity of the measurement series.

We manipulate the regularity of interactions across scales with stochastic multipliers to determine whether reducing this regularity can reshape cascades to yield gradually more cases of $0 < w_{\text{Orig}} < w_{\text{Surr}}$ than $w_{\text{Surr}} < w_{\text{Orig}}$. We will manipulate the variance of the stochastic multipliers and test for differences in one-sample t-statistics expressing the difference between w_{Orig} and a corresponding sample of w_{Surr} for 50 corresponding IAAFT surrogates, that is, t_{MF} defined as the ratio of $(w_{\text{Orig}} - (1/50)\sum_{i=1}^{50} w_{\text{Surr}}(i))$ to the standard error of w_{Surr}. The classic binomial multiplicative cascade of identical interactions across scales unfolds deterministically according to fixed ratio c, and it yields a multifractal spectrum with width $w_{\text{Surr}} < w_{\text{Orig}}$ [21] (e.g., Figure 1) and so positive t_{MF} for a multifractal algorithm that, as we will show, is relatively more likely to generate $0 < w_{\text{Orig}} < w_{\text{Surr}}$. This result suggests

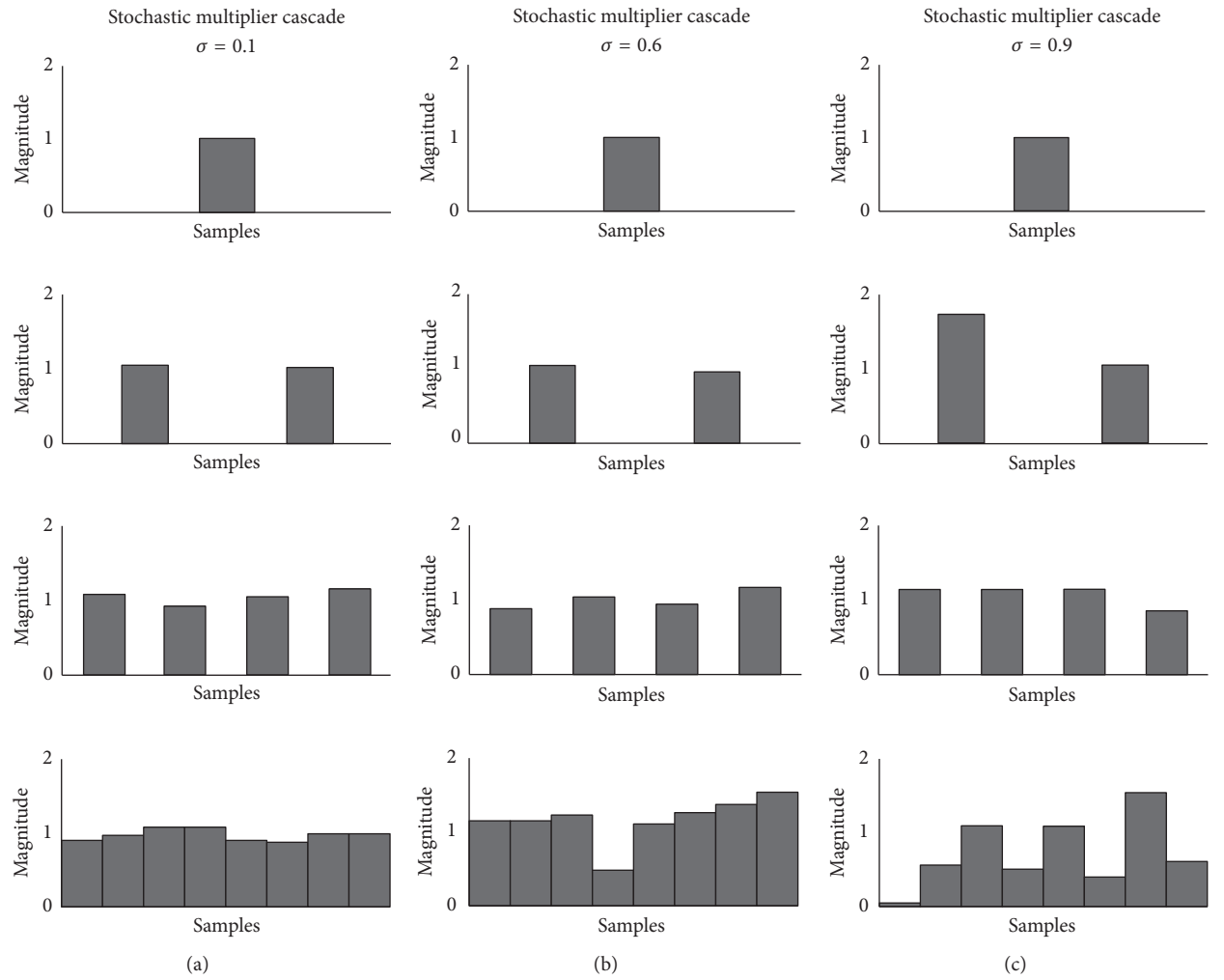

Figure 2: Example of cascades built with two daughter cells replacing each parent cell in each new generation, for $\sigma = 0.1$ (a), 0.6 (b), and 0.9 (c) over the first four generations.

to us that cascades with progressively more heterogeneous interactions across might generate progressively more cases of $0 < w_{\text{Orig}} < w_{\text{Surr}}$ and progressively more negative values of t_{MF}.

We enlist the stochastic multipliers as a means to diversify interactions across scales in the same two-daughter framework. Having only two parameters μ and σ, additive Gaussian white noise offers a simple parameter space for manipulating stochastic multipliers. We defined each new generation j of every cascade with n_j multipliers independently by randomly selecting n_j from a Gaussian distribution with $\mu = 1$. We manipulate the multipliers solely on a between-cascade basis; for example, each cascade will unfold from a process involving multipliers that have the same standard deviation σ across all generations (Figure 2). More elaborate cascade architectures with more free parameters for defining stochastic multipliers might accomplish a similar or even stronger heterogeneity of interactions across scales, but we seek only an existence proof that diversification of interactions across scales will move the distribution of multifractal results significantly much from $w_{\text{Surr}} < w_{\text{Orig}}$ towards $0 < w_{\text{Orig}} < w_{\text{Surr}}$. We predict that cascades generated with greater σ will have a diversity of interactions across scales sufficient to yield a significant increase in series with narrower multifractal spectra than those for corresponding series.

2. Methods

2.1. Generating Simulation Data. We manipulated σ to increase from 0.1 to 1.1, incrementing σ by 0.05 and simulating 200 cascade 12-generation series for each value of σ. In order to control for changes in magnitude with larger σ after iterating 12 generations, we normalized all final series to have mean 10 and standard deviation 1. This final step of normalizing the series to have the same mean and standard deviation entails the notion that the statistical distribution of generated time series is not related to the σ parameter. In other words, for all levels of σ, the generated series all have the same mean and standard deviation.

Other literature on multifractal analysis often uses much longer series [7, 12]. However, our work aims to address

questions about findings appearing in behavioral-science research that draws on multifractal analysis. A frequent constraint of behavioral-science research is shorter series of length much closer to 2^{12} [1]. Hence, our choice of series length was explicitly intended for an attempt to explain what may drive multifractal results in series of this size. However, to test whether significantly negative t_{MF} (i.e., $0 < w_{\mathrm{Orig}} < w_{\mathrm{Surr}}$) might be spuriously due to finite-size constraints on the results of multifractal analysis (e.g., [13]), we drew a sample of series from a previously published dataset [22] for which the average series length was a little more than 2^{16}. We used only those 36 series greater than length of 2^{16}. We do not detail the collection of these series because we only use these series to confirm whether sufficient length makes significantly negative t_{MF} (i.e., $0 < w_{\mathrm{Orig}} < w_{\mathrm{Surr}}$) impossible.

2.2. Multifractal Analysis: MF-DFA Algorithm. MF-DFA integrates a time series $u(t)$ of length N to construct trajectory $y(t)$, as follows:

$$y(t) = \sum_{i=1}^{t} u(i). \tag{1}$$

Linear fits $\widehat{y}(t)$ to $y(t)$ over nonoverlapping windows of length n, $4 \le n \le N/4$, leave residuals contributing to RMS fluctuation statistic $F(n,q)$ growing according to exponent $\alpha(q)$, estimated from $F(n,q)/n$ on double-logarithmic axes:

$$\begin{aligned} F(n,q) &= \left(\frac{1}{N} \sum_{i=1}^{N} \left[\left(y(i) - \widehat{y}_n(i) \right)^2 \right]^{q/2} \right)^{1/q} \\ F(n,q) &\sim n^{\alpha(q)} \\ \log F(n,q) &\sim \alpha(q) \log n. \end{aligned} \tag{2}$$

A Legendre transformation derives multifractal spectrum $(h, D(h))$, as

$$\begin{aligned} h &= \alpha(q) + q\dot{\alpha}(q) \\ D(h) &= q\left[h - \alpha(q)\right] + 1, \end{aligned} \tag{3}$$

where $\dot{\alpha}(q)$ is $d\alpha(q)/dq$. $h_{\max}$–$h_{\min}$ is multifractal-spectrum width w according to MF-DFA [2]. We tested $-20 \le q \le 20$ and included only $\alpha(q)$ for which double-log-scaled $F(n,q)/n$ was linear, $r > 0.95$.

2.3. Multifractal Analysis: Chhabra and Jensen (CJ) Algorithm. Chhabra and Jensen's (CJ) [23] canonical "direct" algorithm samples measurement series $u(t)$ at progressively larger scales. Proportion $P_i(L)$ within bin i of scale L is

$$P_i(L) = \frac{\sum_{k=(i-1)L+1}^{iL} u(k)}{\sum u(t)}. \tag{4}$$

CJ method estimates $P(L)$ for N_L nonoverlapping L-sized bins of $u(t)$ using parameter q to translate them into mass $\mu_i(q,L)$:

$$\mu_{ij}\left(q, L_j\right) = \frac{\left[P_{ij}\left(L_j\right)\right]^q}{\sum_{i=1}^{N_j} \left[P_{ij}\left(L_j\right)\right]^q}. \tag{5}$$

For each q, each estimated $\alpha(q)$ appears in the multifractal spectrum only when Shannon entropy of $\mu(q,L)$ scales with L according to the Hausdorff dimension $f(q)$, where

$$\begin{aligned} f(\alpha(q)) &= -\lim_{N_j \to \infty} \frac{\sum_{i=1}^{N_j} \mu_{ij}\left(q, L_j\right) \ln\left[\mu_{ij}\left(q, L_j\right)\right]}{\ln N_j} \\ f(\alpha(q)) &= \lim_{L_j \to 0} \frac{\sum_{i=1}^{N_j} \mu_{ij}\left(q, L_j\right) \ln\left[\mu_{ij}\left(q, L_j\right)\right]}{\ln L_j} \end{aligned} \tag{6}$$

and where

$$\begin{aligned} \alpha(q) &= -\lim_{N_j \to \infty} \frac{\sum_{i=1}^{N_j} \mu_{ij}\left(q, L_j\right) \ln\left[P_{ij}\left(L_j\right)\right]}{\ln N_j} \\ \alpha(q) &= \lim_{L_j \to 0} \frac{\sum_{i=1}^{N_j} \mu_{ij}\left(q, L_j\right) \ln\left[P_{ij}\left(L_j\right)\right]}{\ln L_j}. \end{aligned} \tag{7}$$

For $-300 \le q \le 300$ and including only linear relationships with correlation coefficient $r > 0.995$ for (6) and (7), the generally single-humped curve $(\alpha(q), f(q))$ is the multifractal spectrum. $\alpha_{\max}$–$\alpha_{\min}$ is multifractal-spectrum width w according to the CJ algorithm.

2.4. Calculating t_{MF} from Comparison to Iterated Amplitude Adjusted Fourier-Transform Surrogates. 50 IAAFT surrogates were produced for each original simulation series, using 1000 iterations of randomizing the phase spectrum from the Fourier transform, taking the inverse-Fourier transform of the original series' amplitude spectrum with the randomized phase spectrum, and replacing the inverse-Fourier series with rank-matched values of the original series. We calculated t_{MF} as the difference $(w_{\mathrm{Orig}} - (1/50)\sum_{i=1}^{50} w_{\mathrm{Surr}}(i))$ divided by the standard error of w_{Surr}. Hence, positive or negative t_{MF} indicated wider or narrower, respectively, spectra than surrogates. We evaluated significance at the $p < 0.05$ level.

Cascades are implicated most directly in nonlinear correlations that appear only partially reflected in the phase spectrum of the Fourier transform, but cascades are not necessary to generate the linear correlations specified by the Fourier transform's amplitude spectrum. Hence, the most rigorous test for identifying cascade processes from multifractal results does require the sample of IAAFT surrogates to preserve both probability distribution function (PDF) and linear correlations [13]. If we were to generate surrogates only by shuffling, that might preserve the PDF but it would not preserve linear correlations, and, in this case, our actual null hypothesis of no cascade-driven nonlinear correlations would be confounded with the null hypothesis of no linear correlations. There may be ample reason to test against the null hypothesis of correlations both linear and nonlinear, but, given that demonstrating cascade-driven origins requires specifically and only nonlinear interactions, then we have no reason to omit linear correlations as an important part of the null hypothesis.

2.5. Regression of Counts for Negative t_{MF}. We modeled the change in frequency of significantly negative t_{MF} using

ordinary least-squares (OLS) regression, fitting a linear term for σ to estimate the effect of incrementing the standard deviation of multipliers, an intercept term for A_{CJ} to estimate the average difference of t_{MF} as calculated by the CJ algorithm rather than the MF-DFA algorithm, and an interaction term $\sigma \times A_{CJ}$ to estimate any differences of t_{MF} calculated by the CJ algorithm in response to incrementing σ.

2.6. Regression of Rank Ordering of All t-Tests. Again using OLS regression, we modeled the change in these distributions with increasing σ by fitting all t_{MF} values as a negative cubic function of rank order,

$$t_{MF} \sim \sum_{i=0}^{3} B_{\text{rank}_i} \times \text{rank}\left(t_{MF}\right)^i, \tag{8}$$

from the highest to the lowest (i.e., most positive to most negative) values of t_{MF}, where B_{rank} is a vector of four regression weights addressing the intercept as well as the linear, quadratic, and cubic components of the third-order polynomial. Visual inspection of rank-ordered t_{MF} indicated that the extreme values on either side of the medians of these distributions were relatively rare, and most values clustered around the median. Cubic approximations are apt for modeling rank-ordered values with these features because the derivative of cubic functions approaches zero near the median values of t_{MF} and increases (or decreases for the negative cubic) at an increasing rate on either side of the origin. We did not explicitly force the cubic term of the regression model to take a negative value. We submitted ranked t_{MF} to a regression model with orthogonalized polynomial terms to ensure that the intercept and linear, quadratic, and cubic terms would not be collinear.

We sought to test whether σ significantly changed the form of the function fit in (8) across all simulations; for example,

$$t_{MF} \sim \sum_{i=0}^{3} B_{\text{rank}_i} \times \text{rank}\left(t_{MF}\right)^i + \sum_{i=0}^{3} B_{\sigma\times\text{rank}_i}\sigma \times \text{rank}\left(t_{MF}\right)^i, \tag{9}$$

where, comparable to B_{rank} introduced in (8), coefficient $B_{\sigma\times rank}$ is a vector of regression weights addressing how the intercept as well as the linear, quadratic, and cubic components of the third-order polynomial changes in ranked t_{MF} with σ. We simultaneously model this cubic relation for t_{MF} calculated using both multifractal algorithms, fitting additional but analogous terms $B_{rank\times CJ}$ and $B_{\sigma\times rank\times CJ}$ to model the difference of t_{MF} between the CJ algorithm and the MF-DFA algorithm.

3. Results

3.1. Increasing σ Increased the Number of Spectra Significantly Narrower Than Corresponding Surrogates. Figure 3 depicts the observed frequencies of significantly negative t_{MF} for each simulated value of σ. Ordinary least-squares (OLS) regression demonstrated that increasing standard deviation σ of the multipliers generating the cascades led to an increase in the number of significantly negative t_{MF}. Specifically, the coefficient in Table 1 for σ of 37.14 indicates that increasing σ of the multipliers by 1 would produce approximately 37 new significantly negative values of t_{MF}. Because we incremented σ by 0.05 for each successive simulation, this coefficient means that, on average, each successive simulation with 0.05-greater σ produced about $1.86 \approx 2$ new negative values of t_{MF}. That amounts to 2 new series, with each incrementing of σ by 0.05, for which $0 < w_{Orig} < w_{Surr}$.

Table 1: Coefficients from regression modeling the frequency of significantly negative t_{MF}.

Predictor	B	SE	p
Intercept	65.76	5.45	<0.0001
σ	37.14	8.11	<0.0001
A_{CJ}	23.50	7.71	<0.01
$\sigma \times A_{CJ}$	−25.27	11.46	<0.05

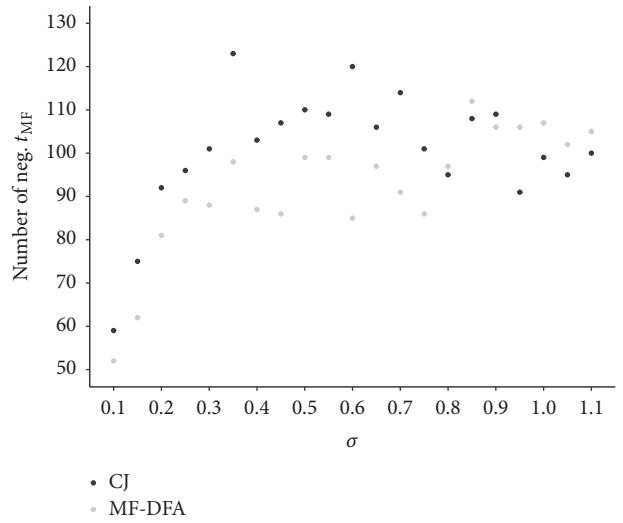

Figure 3: Counts of significantly negative t_{MF} for each σ, according to MF-DFA and by CJ algorithms.

Additional features of the OLS model in Table 1 address the differences by multifractal algorithm. We had applied both MF-DFA and CJ's direct-canonical algorithms. The significant effect of A_{CJ} ($B = 23.50$, SE = 7.71, $p < 0.0001$) indicates that the significantly negative values of t_{MF} were initially more frequent for multifractal spectra calculated using the CJ algorithm. The effect of σ ($B = 37.14$, SE = 6.98, $p < 0.0001$) indicated that the number of negative t_{MF} increased significantly with the increase in σ, by roughly ($37.14 \times 0.05 = 1.86 \approx$) 2 new multifractal spectra in each new simulation with .05 increment in σ. The significant interaction term for $\sigma \times A_{CJ}$ ($B = -25.27$, SE = 11.46, $p < 0.0001$) indicates that the frequency of significantly negative t_{MF} increased much more slowly for multifractal spectra calculated using the CJ algorithm. This slower increase entailed the notion that, for each new simulation incrementing σ by 0.05, the average increase in number of significantly negative t_{MF} is practically negligible ($37.14 \times 0.05 - 25.27 \times 0.05 = 0.5935 \approx 1$).

Table 2: Coefficients from regression modeling the entire distribution of t_{MF}.

Predictor	B	SE	p
Intercept	13.35	0.34	<0.0001
σ	−9.48	0.50	<0.0001
A_{CJ}	−13.83	0.47	<0.0001
$\sigma \times A_{CJ}$	7.90	0.71	<0.0001
Rank (linear)	−1893.25	30.92	<0.0001
Rank (quadratic)	1136.95	30.92	<0.0001
Rank (cubic)	−806.96	30.92	<0.0001
$\sigma \times$ rank (linear)	785.13	46.00	<0.0001
$\sigma \times$ rank (quadratic)	−430.98	46.00	<0.0001
$\sigma \times$ rank (cubic)	315.75	46.00	<0.0001
$A_{CJ} \times$ rank (linear)	1141.30	43.72	<0.0001
$A_{CJ} \times$ rank (quadratic)	−1080.71	43.72	<0.0001
$A_{CJ} \times$ rank (cubic)	653.20	43.72	<0.0001
$\sigma \times A_{CJ} \times$ rank (linear)	−708.45	65.06	<0.0001
$\sigma \times A_{CJ} \times$ rank (quadratic)	354.30	65.06	<0.0001
$\sigma \times A_{CJ} \times$ rank (cubic)	−426.51	65.06	<0.0001

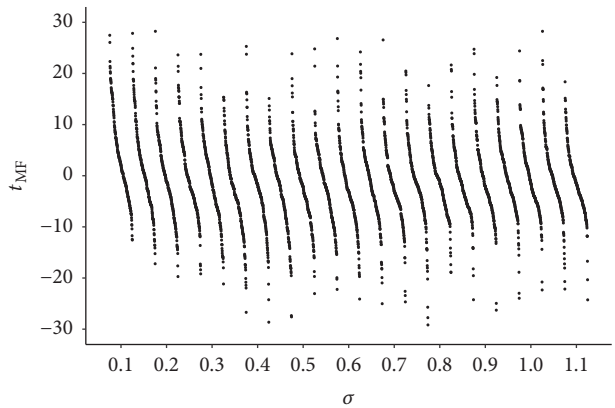

Figure 4: Rank-ordered t_{MF} according to CJ algorithm for each σ.

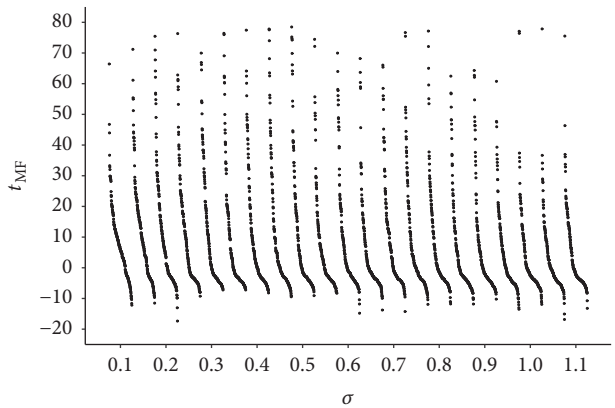

Figure 5: Rank-ordered t_{MF} according to MF-DFA algorithm for each σ.

3.2. Increasing σ Moved and Reshaped the Entire Distribution of t_{MF} for Spectra Calculated Using MF-DFA but Less So for Spectra Calculated Using the CJ Algorithm. Figures 4 and 5 depict both distributions of t_{MF}, with these statistics appearing for spectra calculated using MF-DFA and CJ, respectively. Table 2 contains all individual coefficients from the model described above in (9) and subsequent interactions.

3.3. Intercept Terms Show That Incrementing σ Drives Changes in Median t_{MF} for MF-DFA Algorithm but Slower Changes in Median t_{MF} for CJ Algorithm. Intercept effects in this model address the predicted median t_{MF}. Increasing σ led to a significant reduction ($B = -9.48$, SE = 0.50, $p < 0.0001$) in intercept, suggesting that the median value of t_{MF} calculated using MF-DFA decreased by roughly (9.48×0.05 =) 0.47 with each increment of 0.05 in σ. The model's significant intercept ($B = 13.34$, SE = 0.34, $p < 0.0001$) indicated that the median value of t_{MF} calculated using the MF-DFA algorithm on σ = 0.1 cascades algorithm was roughly (13.34−9.48×0.1 =) 12.39. The significant intercept effect for A_{CJ} ($B = -13.83$, SE = 0.47, $p < 0.0001$) indicated that the median t_{MF} calculated using the CJ algorithm is statistically not different from zero (i.e., 13.34 − 13.83 = −0.49). The significant interaction for $\sigma \times A_{CJ}$ ($B = 7.90$, SE = 0.71, $p < 0.0001$) indicated an increase in t_{MF} calculated using CJ with the increase in σ, counteracting the foregoing negative effect of σ indicating decreases in t_{MF} calculated using MF-DFA. With each 0.05 incrementing of σ, whereas median t_{MF} calculated using the MF-DFA algorithm decreased by 0.47, median t_{MF} calculated using the CJ algorithm decreases by ($-9.48 \times 0.05 + 7.90 \times 0.05$ =) 0.08.

3.4. First- through Third-Order Polynomial Terms Show σ-Dependence of the Entire t_{MF} Distribution for MF-DFA Algorithm but Less for CJ Algorithm. Beyond effects on the predicted median value of t_{MF} all indicated by the intercept terms above, regression modeling confirmed the suitability of a cubic approximation of the entire distributions of ranked values of t_{MF}. The regression model yielded an adjusted

R^2 of 0.72, indicating that this model predicted 72% of the variability in t_{MF}, and as Table 2 shows, all individual effects were significant, $p < 0.0001$. The basic form of the cubic approximation involved a negative cubic term ($B = -806.96$, SE = 30.92, $p < 0.0001$), a positive quadratic term ($B = 1136.95$, SE = 30.92, $p < 0.0001$), and a negative linear term ($B = -1893.26$, SE = 30.92, $p < 0.0001$). The effect of increasing σ served to counteract each component of the basic third-order polynomial (e.g., positive linear and negative quadratic terms, $Bs = 785.13$ and -430.98, both SEs = 46.00, both ps < 0.0001), with the strongest counteraction of this polynomial by σ being a positive cubic term ($B = 315.75$, SE = 46.00, $p < 0.0001$). The interactions of these first- through third-order polynomial terms with A_{CJ} and with $\sigma \times A_{CJ}$ followed were of slightly smaller absolute value but opposite sign of all coefficients corresponding to the linear, quadratic, and cubic terms. These significant but oppositely signed terms indicate that the values of t_{MF} calculated using the CJ algorithm exhibited a similarly cubic term but dramatically less of any change with σ in the shape of the distribution.

Finite-size effect does not explain negative t_{MF} because longer series do not show any diminishing of frequency of negative t_{MF} (i.e., $0 < w_{Orig} < w_{Surr}$). From the 36 series from [22] with length greater than 2^{16}, only 12 of these series yielded significantly wider spectra than their corresponding surrogates, two series were not significantly different, and the remaining 61% of the series yielded significantly narrower spectra than their corresponding surrogates. Against the possibility that there was a systematic change in the frequency of negative t_{MF} with greater length, we found no linear relationship of resulting t statistic with length, $r = 0.014142$.

4. Discussion

We hypothesized that cascades with stochastic multipliers defined as additive white Gaussian noise would produce multifractal spectra significantly narrower than those calculated for their corresponding surrogates. We further hypothesized that increasing the standard deviation σ of stochastic multipliers would increase the number of spectra significantly narrower than for their corresponding surrogates. Results supported this hypothesis, with a greater increase in the number of these narrower-than-surrogates spectra for which $0 < w_{Orig} < w_{Surr}$ as calculated by MF-DFA rather than by the CJ algorithm. The effect of greater standard deviation σ for the stochastic multipliers served not only to change the number of significantly narrower-than-surrogate spectra but also to foster broader migration of the entire distribution of spectra to be narrower than those for corresponding surrogates.

The present work is only a preliminary existence proof in what might be a larger program of cascade simulation manipulating a broader set of parameters. However, we have shown that it does not require elaborate parametrization to produce cascades giving rise to progressively narrower spectra than for corresponding surrogates $0 < w_{Orig} < w_{Surr}$. It is sufficient to introduce stochastic multipliers defined for entire generations into the relatively simple cascade form in which each parent cell gives rise to two daughters in the next generation.

Rather than multifractal analysis only providing a dichotomous diagnosis of cascade structure, the direction of the $w_{Orig} \neq w_{Surr}$ difference might indicate continuous differences in the form of the cascade's interactions across scales.

Competing Interests

The authors declare that there are no competing interests regarding the publication of this paper.

References

[1] E. A. F. Ihlen and B. Vereijken, "Interaction-dominant dynamics in human cognition: beyond $1/f\alpha$ fluctuation," *Journal of Experimental Psychology: General*, vol. 139, no. 3, pp. 436–463, 2010.

[2] J. W. Kantelhardt, S. A. Zschiegner, E. Koscielny-Bunde, S. Havlin, A. Bunde, and H. E. Stanley, "Multifractal detrended fluctuation analysis of nonstationary time series," *Physica A: Statistical Mechanics and Its Applications*, vol. 316, no. 1–4, pp. 87–114, 2002.

[3] S. Lovejoy and D. Schertzer, *The Weather and Climate: Emergent Laws and Multifractal Cascades*, Cambridge University Press, Cambridge, UK, 2013.

[4] B. B. Mandelbrot, *The Fractal Geometry of Nature*, W. H. Freeman and Co., San Francisco, Calif, USA, 1982.

[5] D. L. Turcotte, B. D. Malamud, F. Guzzetti, and P. Reichenbach, "Self-organization, the cascade model, and natural hazards," *Proceedings of the National Academy of Sciences of the United States of America*, vol. 99, no. 1, pp. 2530–2537, 2002.

[6] A. M. Turing, "The chemical basis of morphogenesis," *Philosophical Transactions of the Royal Society of London. Series B. Biological Sciences*, vol. 237, no. 641, pp. 37–72, 1952.

[7] P. Oswiecimka, J. Kwapien, and S. Drozdz, "Wavelet versus detrended fluctuation analysis of multifractal structures," *Physical Review E*, vol. 74, no. 1, Article ID 016103, 17 pages, 2006.

[8] D. P. Mandic, M. Chen, T. Gautama, M. M. Van Hull, and A. Constantinides, "On the characterization of the deterministic/stochastic and linear/nonlinear nature of time series," *Philosophical Transactions of the Royal Society A*, vol. 464, pp. 1141–1160, 2008.

[9] J. Theiler, S. Eubank, A. Longtin, B. Galdrikian, and J. Doyne Farmer, "Testing for nonlinearity in time series: the method of surrogate data," *Physica D: Nonlinear Phenomena*, vol. 58, no. 1-4, pp. 77–94, 1992.

[10] T. Schreiber and A. Schmitz, "Discrimination power of measures for nonlinearity in a time series," *Physical Review E—Statistical Physics, Plasmas, Fluids, and Related Interdisciplinary Topics*, vol. 55, pp. 5443–5447, 1997.

[11] T. Schreiber and A. Schmitz, "Surrogate time series," *Physica D: Nonlinear Phenomena*, vol. 142, no. 3-4, pp. 346–382, 2000.

[12] S. Drożdż, J. Kwapień, P. Oświecimka, and R. Rak, "Quantitative features of multifractal subtleties in time series," *Europhysics letters*, vol. 88, no. 6, Article ID 60003, 2010.

[13] W.-X. Zhou, "Finite-size effect and the components of multifractality in financial volatility," *Chaos, Solitons and Fractals*, vol. 45, no. 2, pp. 147–155, 2012.

[14] Z. R. Struzik, "Econophysics vs. Cardiophysics: the dual face of multifractality," in *The Application of Econophysics*, H. Takayasu, Ed., pp. 210–215, Springer, Tokyo, Japan, 2004.

[15] N. A. Kuznetsov and S. Wallot, "Effects of accuracy feedback on fractal characteristics of time estimation," *Frontiers in Integrative Neuroscience*, vol. 5, article 00062, 2011.

[16] E. A. F. Ihlen, N. Skjæret, and B. Vereijken, "The influence of center-of-mass movements on the variation in the structure of human postural sway," *Journal of Biomechanics*, vol. 46, no. 3, pp. 484–490, 2013.

[17] D. G. Kelty-Stephen and D. Mirman, "Gaze fluctuations are not additively decomposable: reply to Bogartz and Staub," *Cognition*, vol. 126, no. 1, pp. 128–134, 2013.

[18] R. Magrans, P. Gomis, P. Caminal, and G. Wagner, "Multifractal and nonlinear assessment of autonomous nervous system response during transient myocardial ischaemia," *Physiological Measurement*, vol. 31, no. 4, pp. 565–580, 2010.

[19] D. G. Stephen and J. A. Dixon, "Strong anticipation: multifractal cascade dynamics modulate scaling in synchronization behaviors," *Chaos, Solitons and Fractals*, vol. 44, no. 1–3, pp. 160–168, 2011.

[20] T. C. Halsey, M. H. Jensen, L. P. Kadanoff, I. Procaccia, and B. I. Shraiman, "Fractal measures and their singularities: the characterization of strange sets," *Physical Review A*, vol. 33, no. 2, pp. 1141–1151, 1986.

[21] D. G. Kelty-Stephen, K. Palatinus, E. Saltzman, and J. A. Dixon, "A tutorial on multifractality, cascades, and interactivity for empirical time series in ecological science," *Ecological Psychology*, vol. 25, no. 1, pp. 1–62, 2013.

[22] H. S. Harrison, D. G. Kelty-Stephen, D. V. Vaz, and C. F. Michaels, "Multiplicative-cascade dynamics in pole balancing," *Physical Review E—Statistical, Nonlinear, and Soft Matter Physics*, vol. 89, no. 6, Article ID 060903, 2014.

[23] A. Chhabra and R. V. Jensen, "Direct determination of the f(α) singularity spectrum," *Physical Review Letters*, vol. 62, no. 12, pp. 1327–1330, 1989.